

<sup>4</sup>L. P. Kadanoff and A. B. Pippard, Proc. Roy. Soc. (London) A292, 299 (1966).

<sup>5</sup>A. B. Pippard, Proc. Roy. Soc. (London) A257, 165 (1960).

<sup>6</sup>M. H. Jericho and A. M. Simpson, Phil. Mag. 17, 267 (1968).

<sup>7</sup>W. A. Phillips, Proc. Roy. Soc. (London) A309, 259

(1969).

<sup>8</sup>P. A. Bezuglyi, V. I. Denisenko, and V. D. Fil', Zh. Eksperim. i Teor. Fiz. Pis'ma v Redaktsiyu 10, 214 (1969) [Sov. Phys. JETP Letters 10, 134 (1969)].

<sup>9</sup>Tore Olsen, J. Phys. Chem. Solids 24, 187 (1963).

<sup>10</sup>A. B. Pippard, J. G. Shepherd, and D. A. Tindall, Proc. Roy. Soc. (London) A324, 17 (1971).

## Absolute Measurement of the Far-Infrared Surface Resistance of Pb<sup>†</sup>

G. Brändli and A. J. Sievers

*Laboratory of Atomic and Solid State Physics, Cornell University, Ithaca, New York 14850*

(Received 16 December 1971)

The far-infrared surface resistance of Pb has been measured absolutely using a new technique of parallel-plate waveguides. These are made from two rolled-metal foils and a dielectric spacing material or by evaporating the metal directly on both surfaces of the dielectric and thus preventing the air from oxidizing the measured metal surface. Measurements of gold and lead at room temperature show good agreement with the Drude theory and illustrate the accuracy of the new technique. The low-temperature measurements of lead carried out between 6 and 280 cm<sup>-1</sup> in the superconducting and normal state show the onset of the Holstein process (a simultaneous absorption of a photon and emission of a phonon by an electron) and the superconducting energy gap and fit a new sum rule for the surface resistance. The surface resistance of normal Pb agrees well with calculations by Scher, if impurity scattering is taken into account. The data are also compared with Shaw and Swihart's calculations for strong coupling superconductors. The far-infrared properties of the spacing materials, Teflon and polyethylene, used in this work are also given.

### I. INTRODUCTION

The far-infrared absorptivity of Pb at low temperature has recently aroused considerable interest. After Joyce and Richards<sup>1</sup> discovered the onset of the Holstein process<sup>2,3</sup> in a direct absorption experiment, Scher,<sup>4</sup> Allen,<sup>5</sup> and Shaw and Swihart<sup>6</sup> reported calculations based on different theoretical models. Gavini and Timusk<sup>7</sup> repeated the experiment using evaporated Pb in a nonresonant cavity. Both of the experiments are designed for a comparison of the absorptivities in the normal and superconducting state. A quantitative comparison is, however, not possible in these experiments, because the magnetic field used to quench the superconductivity affects the sensitivity of the detectors which are very close to the sample. Joyce and Richards also tried an absolute measurement of the absorptivities of normal and superconducting Pb by a comparison with the absorptivity of carbon. Carbon, however, is not a blackbody in the whole frequency range, and even at the frequencies where it approaches a blackbody the results are only correct up to an unknown scaling factor.

In this paper we report on the first absolute measurements of Pb using a new technique of parallel-plate waveguides. This is a considerable

improvement over the spiral samples used by Drew and Sievers.<sup>8</sup> The results are compared to calculations for normal and superconducting Pb by Shaw and Swihart, based on Nam's<sup>9</sup> theory, and to Scher's calculations for normal Pb. The data also reveal a new sum rule for the surface resistance.

A considerable part of the paper deals with the new technique and some test runs at room temperature: In Sec. II we describe the theory of parallel-plate waveguides, the sample preparation, the details of the measurements, and the properties of the spacing materials; in Sec. III we describe the room-temperature data on Au and Pb. The low-temperature data on Pb and the comparison of the results with theoretical calculations of the Holstein process are presented in Sec. IV.

### II. EXPERIMENTS

#### A. Parallel-Plate Waveguides

The primary component of the samples in this work is a parallel-plate waveguide. The theory of wave propagation between parallel plates or strips is described in many microwave textbooks.<sup>10</sup> The particular configuration which we have used for the far-infrared measurements is briefly re-

viewed here.

We assume that the metallic plates of the parallel-plate transmission line are spaced by a dielectric of thickness  $d$ . If the vacuum wavelength of the applied radiation is larger than  $2dn$ , where  $n$  is the far-infrared index of refraction of the dielectric, only TEM modes are transmitted. TE and TM modes are damped within a distance  $d$  at a vacuum-transmission-line interface and completely reflected as long as the length  $l$  of the line is much larger than  $d$ . The  $E$  and  $H$  vectors in TEM modes are perpendicular to the propagation direction and to each other as for electromagnetic waves in the vacuum. There is only one polarization allowed in the line with the  $E$  vector perpendicular to the plates. When the plates have a finite resistivity, the  $E$  vector has a small component parallel to the wave propagation.<sup>11</sup> We assume a wave propagating as  $e^{i(\omega t - kx)}$  and describe the metal by the frequency-dependent surface impedance,  $Z(\omega) = R(\omega) + iX(\omega)$ , which is also defined when the field-current relation is nonlocal.<sup>12</sup> If we also describe the dielectric medium by the absorption coefficient  $\alpha_D(\omega)$  and the index of refraction  $n(\omega)$ , we find

$$k = \frac{\omega}{c} n(\omega) \left( 1 + \frac{c}{\omega d} \frac{X(\omega)}{Z_0} \right) - i \left( \frac{\alpha_D(\omega)}{2} + \frac{n(\omega)}{d} \frac{R(\omega)}{Z_0} \right) \quad (1)$$

by solving the boundary value problem.<sup>13</sup>  $Z_0 = 4\pi/c$  is the impedance of free space. Equation (1) is linearized under the assumptions  $|Z(\omega)| \ll cZ_0/\omega d$  and  $\alpha_D(\omega) \ll c\omega n(\omega)$ . A somewhat weaker condition,  $|Z(\omega)| \ll Z_0$ , must be fulfilled, so that the fields inside the metal are essentially plane waves propagating perpendicular to the surface. The errors introduced by the above assumptions are at the most about 1% in this work. Within the same accuracy we can neglect the frequency dependence of the far-infrared index of refraction  $n(\omega)$ . This may be checked by applying Kramers-Kronig relations to the measured  $\alpha_D(\omega)$ .

The imaginary part of the surface impedance  $X(\omega)$  gives, according to Eq. (1), an effective index of refraction<sup>14</sup>:

$$n'(\omega) = n \left( 1 + \frac{c}{\omega d} \frac{X(\omega)}{Z_0} \right) \quad (2)$$

The imaginary part of  $k$  describes the attenuation of a TEM wave in the line. The intensity is attenuated by the factor  $e^{-2 \operatorname{Im}(k)x}$ . Thus the transmitted intensity  $I(\omega)$  for a line of length  $l$  and with reflection coefficient  $r(\omega)$  at the two ends is

$$I(\omega) = I_0(\omega) [1 - r(\omega)]^2 \exp \left[ - \left( \alpha_D(\omega) + \frac{2n}{d} \frac{R(\omega)}{Z_0} \right) l \right], \quad (3)$$

assuming multiple internal reflections to be negligible.

### B. Array of Parallel Plates

Because the optics of our far-infrared interferometer have a wide-angle aperture, it is not possible to focus the radiation onto the small slit of one parallel-plate transmission line without losing most of the intensity. We have constructed a parallel array of several hundred lines which form a better match to our optical system. We now discuss its special properties.

Carlson and Heins<sup>15,16</sup> calculated the transmission and reflection coefficient for an electromagnetic plane wave at a number of parallel metallic plates of zero thickness and perfect conductivity. The plates are assumed equally spaced, positioned at  $z = 0, \pm a, \pm 2a, \text{ etc.}$ , and filling the half-space  $x > 0$ . The incident wave propagates in the  $xz$  plane in a direction  $\theta$  with respect to the  $x$  axis. If the vacuum wavelength  $\lambda_0$  is larger than  $a(1 + \sin\theta)$ , no diffraction effects exist, i.e., there is only one reflected wave. If  $\lambda_0 > 2a$ , only one polarization is transmitted: The plates are perfect mirrors for waves with the  $E$  vector parallel to them.<sup>15</sup> Waves with a perpendicular  $E$  vector are transmitted as TEM modes.<sup>16</sup> The coefficient for the reflected intensity  $r = (1 - \cos\theta)^2 / (1 + \cos\theta)^2$ , is small, independent of the frequency  $\omega$ , and disappears at normal incidence.

In analogy with these exact results, the reflection and transmission characteristics of our samples can now be derived. Our samples have a dielectric space between the metallic plates, and the metal has a finite thickness  $d_m$  and a finite conductivity. This leads to an enhanced index of refraction [Eq. (2)] and reflection coefficient. The incident radiation is within a cone of half-apex angle  $\theta_{\max} = 0.3$  rad ( $18^\circ$ ) and has an essentially unknown angular distribution. Thus, the reflection coefficient in Eq. (3) is calculated to be  $r = [(n' - 1)^2 / (n' + 1)^2] (1 + \beta \theta_{\max}^2)$  and, except for  $n'$ , is independent of the frequency.<sup>17</sup> Here  $\beta \approx 0.3$  estimates the influence of all the incident waves with  $\theta \neq 0$ . Since the important parameter in Eq. (3) is  $(1 - r)$ , we can state well within the 1% error of our calculation that  $n' = n$  and  $\beta = 0$  and find the transmitted intensity of an array of plates to be

$$I(\omega) = I_0^+(\omega) \left( \frac{d}{d + d_m} \right)^2 \left[ 1 - \left( \frac{n - 1}{n + 1} \right)^2 \right]^2 \times \exp \left[ - \left( \alpha_D(\omega) + \frac{2n}{d} \frac{R(\omega)}{Z_0} \right) l \right], \quad (4)$$

where  $I_0^+(\omega)$  is the incident radiation having the  $E$  vector perpendicular to the plates and the factor  $d/(d + d_m)$  takes the shadowing effect of the metallic plates into account. Two conditions have to be

fulfilled:  $\lambda_0 > (d + d_m)(1 + \sin\theta_{\max})$  for no diffraction effects, and  $\lambda_0 > 2dn$  for TEM modes only. From the results by Collin<sup>18</sup> it can be concluded that a plane wave of oblique incidence entering an array of plates of length  $l \gg d$  leaves the plates at  $x=l$  at the original angle. In other words, the angular distribution of the incident radiation is restored after the transmission.

### C. Sample Preparation and Measuring Principles

We either prepared strips of dielectric film and rolled metallic foil of about 2-cm width or evaporated the metal on both sides of a dielectric film of about 30×30-cm area and cut this into strips. The strips were wound around a thin brass plate as shown in the upper half of Fig. 1. Two thicker plates pressed the roll flat against the thin plate (lower half of the figure). The surplus material was removed and the roll cut in two samples of different length by a thin saw. The cross sections of the samples were at least 1 cm<sup>2</sup>. They actually had about four thin brass plates instead of one as shown in Fig. 1. The surfaces of the samples were made plane and smooth by a dry sanding on

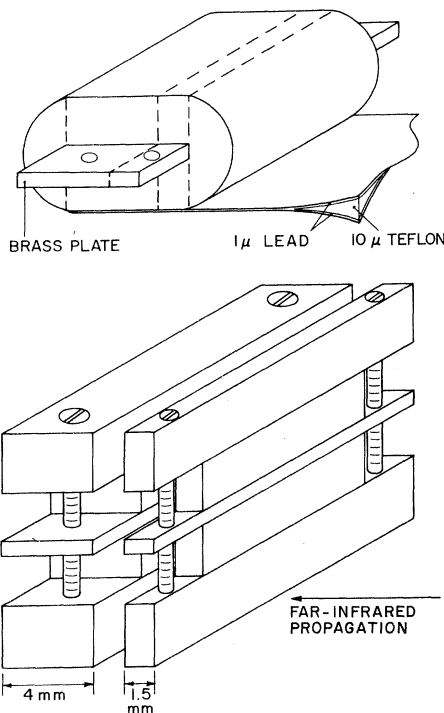


FIG. 1. Preparation of two transmission-line samples. The spacing material Teflon covered with two layers of evaporated Pb is wound around a thin brass plate. The roll is then pressed between thicker brass plates, cut apart along the dashed lines with the round ends removed to get two samples of equal cross sections but different lengths.

emery paper. Interference fringes in the short sample were overcome by tilting one end plane slightly with respect to the other. Radiation leakage out the sides of the samples was prevented by a circular mask that reduced the area of the incident radiation so that all the transmitted intensity was collected.

The ratio of the transmitted light intensities for the two samples is calculated from Eq. (4) to be

$$\frac{I(\omega, l_1)}{I(\omega, l_2)} = \exp \left[ - \left( \alpha_D(\omega) + \frac{2n}{d} \frac{R(\omega)}{Z_0} \right) (l_1 - l_2) \right]. \quad (5)$$

Note that the unknown  $I_0^t(\omega)$  and the reflection coefficients drop out. The measurement of  $\alpha_D(\omega)$  was done by preparing two samples as in Fig. 1 from the pure dielectric film. Care was taken to wind the film in the same direction as for the metallic samples, because most dielectric films are not isotropic. The transmitted intensity of a pure dielectric sample is given by

$$I(\omega) = I_0^t(\omega) \left[ 1 - \left( \frac{n-1}{n+1} \right)^2 \right]^2 \exp[-\alpha_D(\omega)l], \quad (6)$$

and the ratio of two pure dielectric samples of different lengths is

$$I(\omega, l_1)/I(\omega, l_2) = \exp[-\alpha_D(\omega)(l_1 - l_2)]. \quad (7)$$

Having determined  $n$  from interference fringes in a short pure dielectric sample a measurement of  $R(\omega)/Z_0$  is possible by dividing the intensities of a metallic and pure dielectric sample of equal lengths [Eqs. (4) and (6)]:

$$I_{\text{metal}}(\omega)/I_{\text{p.d.}}(\omega) = \gamma \frac{d}{d + d_m} \exp \left( - \frac{2n}{d} \frac{R(\omega)}{Z_0} l \right), \quad (8)$$

where the correction factor  $\gamma$ , which takes into account changes in the effective cross sections of the samples, has to be determined experimentally. This factor also does not seem to be completely frequency independent.<sup>17</sup>

A better method, which has been adopted for this work, is to use four samples and to deduce  $R(\omega)/Z_0$ , which is also approximately equal to  $\frac{1}{4}$  of the absorptivity, from Eqs. (5) and (7) without fitting any parameter. The samples were mounted on a sample rotator along the light pipe (12.7-mm brass tube) between the interferometer and the detector. We used a lamellar-grating interferometer below 50 cm<sup>-1</sup> and a Michelson interferometer between 30 and 300 cm<sup>-1</sup> with Ge bolometers cooled to 0.4 and 1.2°K, respectively.

### D. Properties of the Spacing Materials

A very good spacing material is Teflon, which is available as high-quality films<sup>19</sup> with thicknesses down to  $d = 3 \mu\text{m}$ . The evaporation of metal layers on this substrate is quite straight-

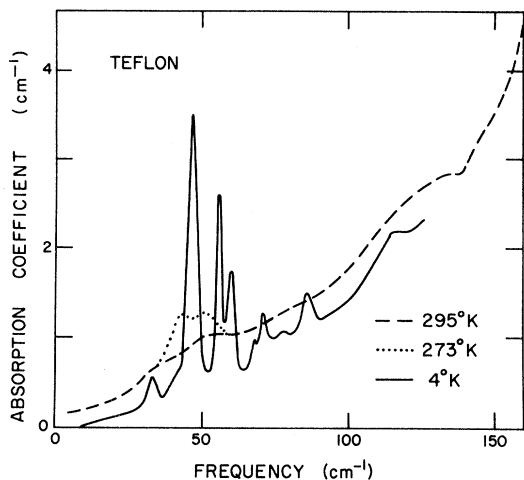


FIG. 2. Absorption coefficient of Teflon. Teflon is a good spacing material up to  $150 \text{ cm}^{-1}$  at room temperature but has some very disturbing bands at low temperatures that reduce the useful range for most applications down to frequencies below  $30 \text{ cm}^{-1}$ .

forward and the metal layers may be annealed at temperatures up to  $300^\circ\text{C}$ . The absorption coefficient of Teflon is plotted versus frequency from  $5$  to  $150 \text{ cm}^{-1}$  in Fig. 2. There is a strong absorption band at about  $220 \text{ cm}^{-1}$  that makes Teflon opaque for the purpose of this work at frequencies higher than  $150 \text{ cm}^{-1}$ .

The Teflon molecules have a spiral structure which undergoes a first-order phase transition at  $19^\circ\text{C}$ . At lower temperatures some new bands appear which are very sensitive to strain. Metals and the dielectrics used in this work have very different thermal-expansion coefficients. The dielectric in the composite samples can fully contract only in one dimension. Strains build up which shift the absorption bands to frequencies different from their position in the unstrained dielectric. The  $\alpha$ 's in Eqs. (5) and (7) no longer agree and cannot be divided out. We have concluded that the use of Teflon as a spacing material at low temperatures is only practical for frequencies below  $30 \text{ cm}^{-1}$ .

The other spacing material used in this work is a commercial "all-purpose polyethylene sheet" of about  $6 \mu\text{m}$  showing varying thickness and unknown origin and composition. The absorption coefficient of this material is shown in Fig. 3. It has an absorption band at  $79 \text{ cm}^{-1}$  as reported for low- and high-density polyethylene,<sup>20</sup> but the bands at  $114$  and  $237 \text{ cm}^{-1}$  are of unknown origin. This film had to be cooled to liquid-nitrogen temperature for the evaporation of Pb. Annealing is possible up to about  $85^\circ\text{C}$ .

The absorption bands and the far-infrared index

of refraction of both spacing materials are given in Table I. We have chosen the thickness of the spacing for all samples of this work so thin that the absorption in the spacing material remains below the absorption at the metallic surfaces [Eq. (3)] even at the band frequencies. Considerable improvement in the transmission-line technique is still possible with better spacing materials or evaporating multilayers of metal and spacers.

### III. ROOM-TEMPERATURE RESULTS OF Au AND Pb

Before applying the new technique to metals with an unknown surface resistance, we wanted to test it on simple systems to get some feeling for the accuracy of the Fourier-transform techniques. Figure 4 shows the results for a room-temperature measurement of Au. The best results were obtained with a rolled and annealed gold foil of  $8\text{-}\mu\text{m}$  thickness. Its residual dc resistivity was measured as  $\frac{1}{16}$  of the room-temperature resistivity. Using a literature value for this, the dc resistivity was found to be  $\rho_0 = 2.3 \mu\Omega\text{cm} = 2.55 \times 10^{-18} \text{ sec}$ . The Drude theory<sup>21</sup> (excluding relaxation) predicts  $R(\omega)/Z_0 = \frac{1}{2}(\omega\rho_0/2\pi)^{1/2}$  for the surface resistance, where the frequency  $\omega$  is given in  $\text{sec}^{-1}$  and  $\rho_0$  in sec. Although this theory does not hold for Au at room temperature up to  $150 \text{ cm}^{-1}$ , the relaxation and anomalous skin effects accidentally cancel each other so that the correct free-electron result from Dingle's table<sup>22</sup> as given by a full line in the figure is very close to the Drude prediction. The difference found between experiment and theory (curves C and D) might be due to an enhanced impurity concentration in the surface layer of the rolled Au foil. An attempt to get better results by evaporating the gold ( $1000 \text{ \AA}$  thick, 99.9% purity) failed. The necessary annealing could not be done

TABLE I. Absorption bands and far-infrared index of refraction for the two spacing materials used in this work. *a*, *b*, and *c* indicate strong, medium, and weak bands, respectively.

	Teflon		Polyethylene	
	300 °K	4.2 °K	300 °K	4.2 °K
Absorption bands		$33.5^b \text{ cm}^{-1}$	$76^b \text{ cm}^{-1}$	$79^b \text{ cm}^{-1}$
		$46.5^a$	$117^a$	$114^a$
		$56^a$		
		$60^a$	$230^a$	$237^a$
		$68^c$		
		$71^b$		
		$78^c$		
	$86^b$			
	$116^c$			
Index of refraction	$1.42 \pm 0.02$		$1.52 \pm 0.02$	

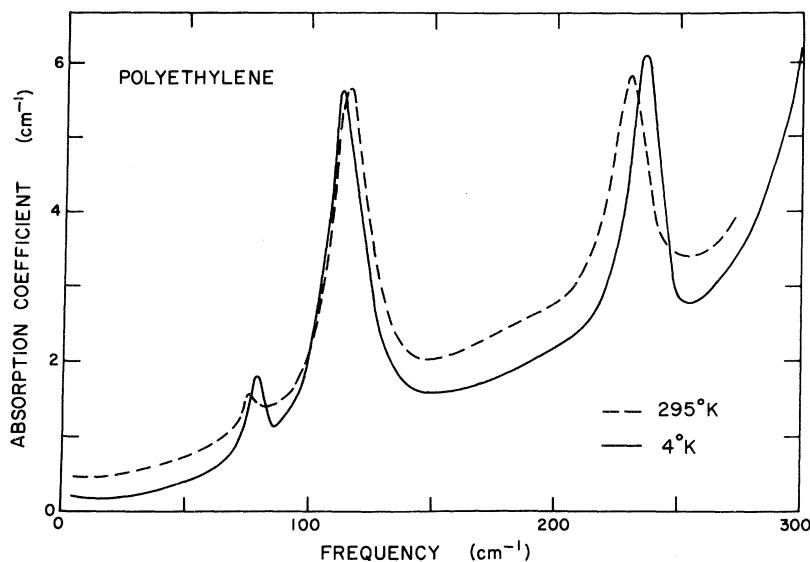


FIG. 3. Absorption coefficient of all-purpose polyethylene. This material can be used for spacing up to  $300 \text{ cm}^{-1}$  at room and low temperatures. It has a variable thickness and other disadvantages mentioned in the text.

because of the low melting point ( $326^\circ\text{C}$ ) of Teflon. The pure-Teflon samples were submitted to the same vacuum annealing as the composed samples.

The results for Pb are plotted in Fig. 5. Curve A was measured on a rolled Pb foil of  $25\text{-}\mu\text{m}$  thickness that was stored in air for months and had a thick oxide layer.<sup>23</sup> The best results were obtained with evaporated Pb ( $1\text{-}2 \mu\text{m}$  thick) and annealed

Pb (curve C). The low-frequency data are measured on a different pair of samples using  $10\text{-}\mu\text{m}$  Teflon films. No systematic deviation was found

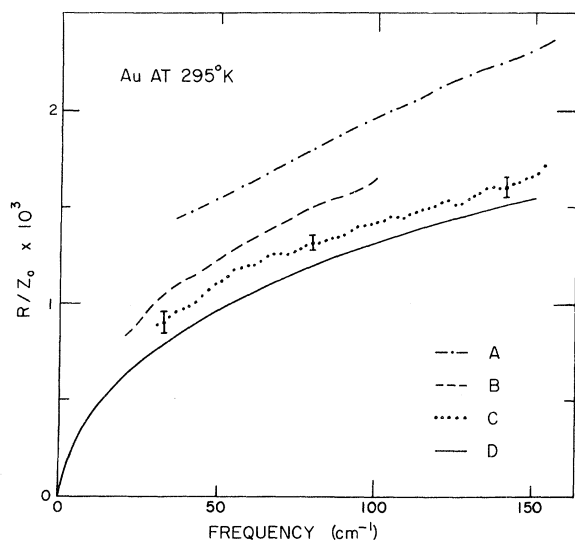


FIG. 4. Surface resistance of Au at room temperature. A stands for evaporated, but unannealed gold; B, same samples annealed for three days at  $300^\circ\text{C}$ ; C, rolled and annealed gold foil; D, calculated from Dingle's table using the measured dc resistivity of C. The spacing material was  $10\text{-}\mu\text{m}$  Teflon film for all samples.

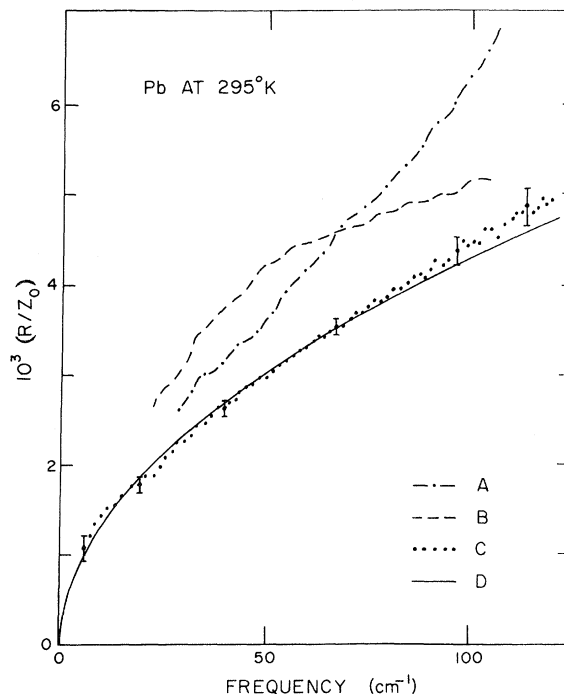


FIG. 5. Surface resistance of Pb at room temperature. A, rolled lead foil; B, evaporated but unannealed lead; C, same samples as B annealed for 18 h at  $250^\circ\text{C}$ ; D, Drude theory based on the dc resistance of C (no fitted parameter!). The spacing material was  $25\text{-}\mu\text{m}$  Teflon film.

in the overlapping region between 30 and 50  $\text{cm}^{-1}$ . Lead at room temperature is such a poor conductor that the Drude theory is exact. The only parameter in this theory, the dc resistivity, was determined to be  $\rho_0 = 2.45 \times 10^{-17}$  sec from the resistivity ratio of  $\frac{1}{43}$  and the literature value of the room-temperature resistivity (21.5  $\mu\Omega$  cm). The agreement between experiment and theory (curves C and D) is very good except at the highest frequencies, where the samples have become nearly opaque. The deviation might be caused by a small error in the zero level of the transmitted intensity or by the roughness of the Teflon-Pb interface, which has in general a remarkably small influence.

#### IV. LOW-TEMPERATURE RESULTS ON Pb

The surface resistance of normal and superconducting Pb was measured with the polyethylene film described above. 1–2  $\mu\text{m}$  of Pb (Cominco 99.999% pure) were evaporated from a tantalum boat in a vacuum of  $10^{-6}$  Torr. This thickness of Pb already has bulk properties. The polyethylene substrate was cooled to liquid-nitrogen temperature during evaporation. The thickness of the polyeth-

ylene varied from 5 to 8  $\mu\text{m}$ . The average thickness was determined to be 5.8  $\mu\text{m}$  from a fit of the room-temperature surface resistance to the Drude theory. A polyethylene film of this thickness and covered with 1–2  $\mu\text{m}$  of Pb on each side can fully contract in only one dimension when cooled so that the polyethylene is strained. This shifts its three bands (Fig. 3) in frequency with respect to the unstrained sample. We have shifted the bands rigidly back until the surface resistance in the normal state ( $R_N$  in Fig. 6) is smoothly varying with frequency at the band frequencies. The corrected points are identified with smaller dots. The  $R_S$  data were then calculated using the differences  $R_S - R_N$  (Fig. 7), which, of course, are not affected by the band shifts. Strains built up in the Pb are so small that their effects can be neglected in comparison to other experimental errors.

The data on normal Pb were taken at 8°K (the critical temperature was measured to be 7.18°K). At this temperature some low-energy phonons are already excited, but there is a smaller volume change than if the superconductivity is quenched by a magnetic field. Also the problem of magneto-resistance and trapped flux are eliminated. The last point is experimentally important, because it allows one to measure the two states in repetition and keep track of drifts. The data on normal Pb ( $R_N$ ) are shown in Fig. 6. The only pronounced structure is an apparent small dip at 25  $\text{cm}^{-1}$  which is well established from high-resolution runs made at low frequencies.<sup>24</sup> The dip at 25  $\text{cm}^{-1}$  is where the phonon density of states increases sharply<sup>25</sup> and must be the onset of the Holstein process.<sup>2</sup>

Scher<sup>4</sup> and Allen<sup>5</sup> calculated  $R_N$  by solving the Holstein-Boltzmann equation.<sup>26</sup> Their numerical results are quite similar although they use different values for the Fermi velocity and treat the "scattering-in" terms differently, so that Allen's calculation should be equivalent to that by Shaw and Swihart<sup>6</sup> (curve B). This calculation is based on Nam's<sup>9</sup> theory for strong coupling superconductors under addition of the Holstein relaxation mechanism. Scher's numerical result is plotted as curve C in Fig. 6. We multiplied it by a factor of  $\frac{9}{8}$ , because the diffuse surface scattering of the electrons is adequate for the rough Pb-polyethylene interface of our samples, and we used the relationship  $A \approx 4R/Z_0$ , where  $A$  is the absorptivity. Scher finds an extra contribution to the extreme anomalous skin effect from the "scattering-in" terms. This can be described by a mass renormalization and leads to the flat section around 30  $\text{cm}^{-1}$  in curve C. The barely visible positive curvatures at about 35 and 67  $\text{cm}^{-1}$  correspond to peaks in the phonon density of states. Scher<sup>4</sup> showed in a private communication how the extra absorption due to the impurity scattering can be

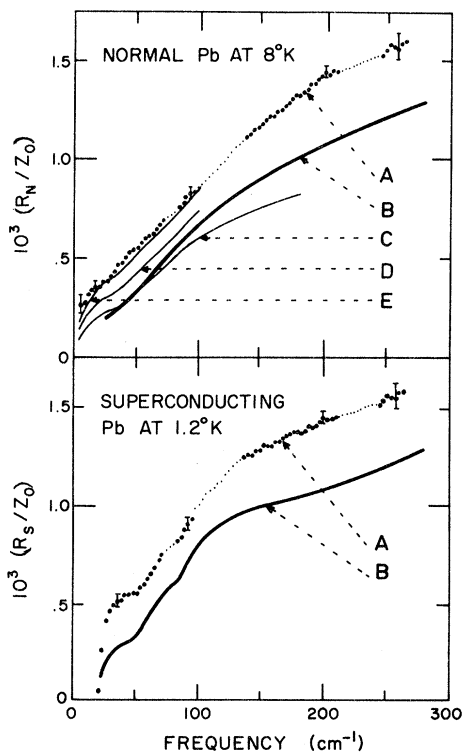


FIG. 6. Surface resistance of Pb in the normal and superconducting state. A, lead evaporated on 6- $\mu\text{m}$  polyethylene and annealed for 3½ days at 85°C; B, theoretical calculations by Shaw and Swihart. C, D, and E are adaptations of Scher's calculations to our samples as discussed in the text.

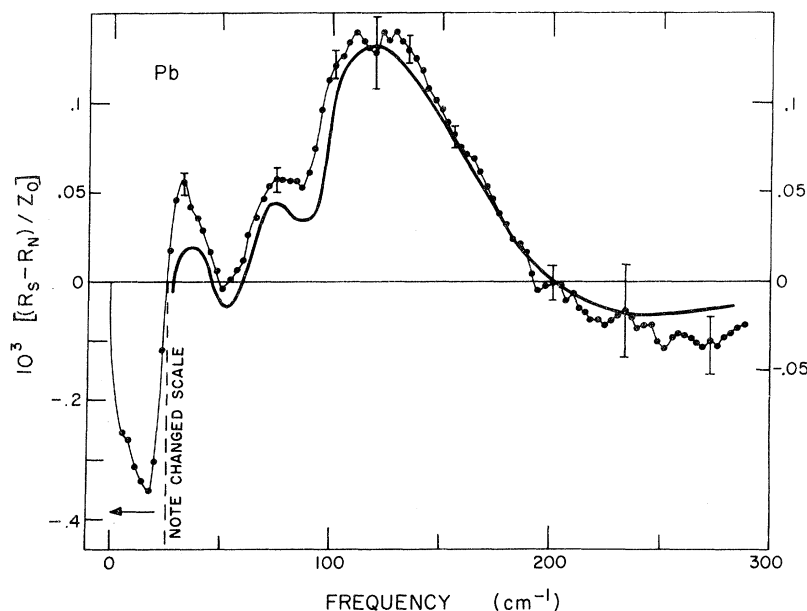


FIG. 7. Difference of the surface resistances of Fig. 6. Note the three times smaller scale for  $(R_N - R_S)$  at frequencies below  $26 \text{ cm}^{-1}$ . The measurements are on an absolute scale and agree very well with the calculations by Shaw and Swihart (Ref. 6). The areas above and below the zero level cancel. This leads to a new sum rule.

included in his results. For frequencies below  $100 \text{ cm}^{-1}$ , one gets the extra absorption  $\delta A_{\text{imp}}$  by setting it equal to the second term in the Dingle series expansion and replacing  $i\Omega$  by  $1/\tau$ , where  $\tau$  is the relaxation time of the electrons. We found that  $\tau = 1.9 \times 10^{-13}$  sec from the measured dc resistivity of our samples and the band parameters used by Scher. This yields  $\delta R_{\text{imp}}/Z_0 = 0.027 \times 10^3 \omega^{1/3} (\text{cm}^{-1})$  and, when added to the calculations for pure Pb, curve D. An impurity concentration twice as high as measured (curve E) would lead to a good agreement with the data. Because the far-infrared radiation penetrates only about  $\frac{1}{30}$  of the evaporated Pb layer, which could not be annealed at a sufficiently high temperature, it is quite probable that the discrepancy is due to a higher impurity concentration in the surface layer compared to the measured bulk value. In any case, the data show that Scher's extra term to the extreme anomalous skin effect is necessary to explain the surface resistance below  $30 \text{ cm}^{-1}$ .

The data for the superconducting lead  $R_S$  show the energy gap at  $21 \text{ cm}^{-1}$  and the steps of the Holstein process<sup>26</sup> at about  $55$  and  $90 \text{ cm}^{-1}$ . These latter frequencies correspond to the peak energies in the phonon density of states shifted upwards by the energy-gap frequency. Then only the difference between the photon and gap energies is available for a phonon emission in the Holstein process. The sharper steps in the superconducting state are due to electron-pair correlations and the sharp peaks in the electron density of states near the gap. The data show a sharp rise of  $R_S$  just above the energy-gap frequency; this is correctly given by Swihart and Shaw<sup>27</sup> in contrast to the slow in-

crease calculated by Mattis and Bardeen<sup>28</sup> in the weak coupling limit.

Figure 7 shows the difference  $[R_S(\omega) - R_N(\omega)]$ . These data are not affected by strain-induced frequency shifts of the polyethylene absorption bands, because the small change in temperature does not alter the strains, but nevertheless have an increased noise at the band frequencies due to a lower transmitted intensity. The data contain all the fine structure of the phonon density of states as first found by Gavini and Timusk.<sup>7</sup> The thick solid line is the calculation by Shaw and Swihart<sup>6</sup> based on tunnel-effect measurements of the phonon density of states and does not include all its details. The agreement between our data and their calculation (neither contains fitted parameters) is very good.

The  $[R_S(\omega) - R_N(\omega)]$  data of Fig. 7 also reveal that the areas above and below the zero level are equal within the experimental errors (note the changed scale for frequencies lower than  $26 \text{ cm}^{-1}$ ), i. e., this is a sum rule for the surface resistance requiring

$$\int_0^\infty [R_S(\omega) - Z_0] d\omega = \int_0^\infty [R_N(\omega) - Z_0] d\omega \quad (9)$$

This new sum rule can be understood from a Kramers-Kronig argument. It reveals an inherent connection between the Holstein process and superconductivity, which both depend on the phonon density of states and the electron-phonon matrix element, because  $R_S$  exceeds  $R_N$  at the phonon frequencies, where the Holstein process begins. The sum rule has been reported previously and proved also for two In-Pb alloys.<sup>29</sup>

## V. CONCLUSIONS

The new technique gives good data for rolled metals with a clean surface (e.g., Au) or evaporated metals, when annealing is possible (Pb). Storage of the samples for months in air does not affect the reproducibility of the data. The samples are measured in transmission and can be placed far removed from the detector in a different environment.

We presented here the first absolute measurements of the surface resistance of metals in the far infrared. The low-temperature data on lead show all the theoretically predicted structure in the frequency dependence, but disagree in mag-

nitude. If, however, the impurity concentration near the surface is assumed to be twice as high as measured for the bulk film, a good agreement is found within the estimated errors.

## ACKNOWLEDGMENT

We wish to thank Dr. H. Scher for communicating and discussing the extra surface resistance term due to impurity scattering and Professor J. C. Swihart and Dr. W. Shaw for communicating their results prior to publication. Many helpful discussions with S. R. Derbenwick, D. G. B. Tanner, R. K. Elsley, and A. B. Bringer are gratefully acknowledged.

<sup>†</sup>Work supported by the U.S. Atomic Energy Commission, under Contract No. AT(11-1)-3151, Technical Report No. CH-3151-136. Additional support was received from the Advanced Research Projects Agency through the Materials Science Center at Cornell University, Report No. 1680.

<sup>1</sup>R. R. Joyce and P. L. Richards, Phys. Rev. Letters 24, 1007 (1970).

<sup>2</sup>T. Holstein, Phys. Rev. 96, 535 (1954).

<sup>3</sup>M. A. Biondi, Phys. Rev. 96, 534 (1954).

<sup>4</sup>H. Scher, Phys. Rev. Letters 25, 759 (1970); Phys. Rev. B 3, 3551 (1971).

<sup>5</sup>P. B. Allen, Phys. Rev. B 3, 305 (1971).

<sup>6</sup>W. Shaw and J. C. Swihart, Bull. Am. Phys. Soc. 16, 352 (1971).

<sup>7</sup>A. Gavini and T. Timusk, Phys. Rev. B 3, 1049 (1971).

<sup>8</sup>H. D. Drew and A. J. Sievers, Phys. Rev. Letters 19, 697 (1967).

<sup>9</sup>S. B. Nam, Phys. Rev. 156, 470 (1967).

<sup>10</sup>See, e.g., J. C. Slater, *Microwave Transmission* (McGraw-Hill, New York, 1942), p. 138.

<sup>11</sup>The  $E$  vector turns completely into the plane of the plates when entering the metal. This might be of interest for Azbel'-Kaner resonance measurements.

<sup>12</sup>L. D. Landau and E. M. Lifshitz, *Electrodynamics of Continuous Media*, 2nd ed. (Pergamon, New York, 1966), p. 280.

<sup>13</sup>H. D. Drew, A. J. Sievers, G. Brändli, and S. Derbenwick (unpublished).

<sup>14</sup>We have tried to measure  $n'$  by studying the standing waves in a short waveguide with exactly parallel ends. When the term with  $X$  is large, however, the term with  $R$  is large too and reduces the amplitude of the standing wave. No difference between  $n$  and  $n'$  could be detected.

<sup>15</sup>J. F. Carlson and A. E. Heins, Quart. Appl. Math. IV, 313 (1947).

<sup>16</sup>A. E. Heins and J. F. Carlson, Quart. Appl. Math. V, 82 (1947).

<sup>17</sup>Some experiments suggest that  $r$  increases slightly but smoothly with the frequency  $\omega$  for the samples of this work.

<sup>18</sup>R. E. Collin, *Field Theory of Guided Waves* (McGraw-Hill, New York, 1960), p. 430.

<sup>19</sup>Fluorofilm (trademark of the Dielectric Corp., Farmingdale, New York).

<sup>20</sup>N. W. B. Stone and D. Williams, Appl. Opt. 5, 353 (1966).

<sup>21</sup>See, e.g., B. Donovan, *Elementary Theory of Metals* (Pergamon, New York, 1967), p. 218.

<sup>22</sup>R. B. Dingle, Physics 19, 311 (1953).

<sup>23</sup>An exact calculation of the wave propagation of a parallel-plate transmission line, with the metallic plates covered with a thin oxide layer, yielded no enhanced absorption for reasonable parameters as long as the surface layer does not have a reststrahlen band at the frequencies of interest. This is probably the case for curve A, which continued to increase very steeply up to  $130 \text{ cm}^{-1}$ .

<sup>24</sup>Our data do not show the negative slope at  $150 \text{ cm}^{-1}$  as found by Joyce and Richards (Ref. 1) which may be caused by a frequency dependence in the carbon absorptivity. An interband transition between the third and fourth zones of the Fermi surface at  $33 \text{ cm}^{-1} = 4 \text{ meV}$  [J. R. Anderson and D. C. Hines, Phys. Rev. B 2, 4752 (1970)] has not been detected.

<sup>25</sup>J. M. Rowell, W. L. McMillan, and W. L. Feldmann, Phys. Rev. 178, 897 (1969).  $25 \text{ cm}^{-1}$  correspond to  $3.1 \text{ meV}$ , where  $\alpha^2 F$  of Pb rises sharply.

<sup>26</sup>T. Holstein, Ann. Phys. (N. Y.) 29, 410 (1964).

<sup>27</sup>J. C. Swihart and W. Shaw, Physica (to be published).

<sup>28</sup>D. C. Mattis and J. Bardeen, Phys. Rev. 111, 412 (1958).

<sup>29</sup>G. Brändli, Phys. Rev. Letters 28, 159 (1972).